# THEORETICAL STUDY OF BOILING HEAT TRANSFER IN A THIN FILM ON HORIZONTAL TUBE

# دراسه نظرية لانتقال الحراره بالغليان فى طبقة رقيقة على أنبوبة أفقية

**M. G. WASEL , A. A. KAMEL , H. M. MOSTAFA**
*Mechanical Power Engineering Department*
*Faculty of Engineering , El-Mansoura university*

خلاصه: في هذا البحث تم دراسه ظاهره انتقال الحراره المصاحب للغليان على انبوبه افقيه واشتملت هذه الدراسه بحث دور كل من العوامل المؤثره فى عمليه انتقال الحراره - مثل الفيض الحرارى ومعدل السريان وقطر الانبوبة على معامل انتقال الحراره . تم حل النموذج الرياضى الواصف لهذا السريان عدديا بطريقه الفروق المحدده وذلك بتصميم وتنفيذ برنامج للحاسب الالي . باستخدام هذا النموذج امكن الحصول على توزيع درجات الحراره خلال الطبقه الملاصقه للجدار الخارجي للانبوبه و من ثم تم حساب معامل انتقال الحراره عند الظروف المؤثره المختلفه . لاختبار صلاحيه هذا النموذج المقترح تم مقارنه النتائج المستخلصه منه مع مثيلاتها من الابحاث السابقه . هذا البحث درس انتقال الحراره لانابيب ذات قطر ١٢ , ١٩ , ٣٨ مم وكان مدى رقم رينولدز من ١٠٠ الى ٥٠٠ ، و مدى فرق درجات الحراره يصل الى ٣٥ درجة مئوية .

## ABSTRACT

Boiling heat transfer process in a thin film on horizontal tube is ,theoretically, investigated . This subject is important for design of the horizontal tube evaporator- condenser (HTE) , which is applied in distillation processes. The effect of the operating parameters ( heat flux, mass flow rate and tube diameter ) is investigated . To perform this study , a theoretical model is proposed, and a computer program is developed to solve this model numerically. This program is used to determine local and average boiling heat transfer coefficient for different operating parameters in laminar flow regime. The range of Reynolds number is taken as 100-500 and wall superheat up to 35 °C. The diameter of tested tube was 12, 19 and 38 mm.

## 1- INTRODUCTION

Heat transfer through falling-film or spray-film evaporation has been widely employed in heat exchange devices in the chemical, refrigeration, petroleum refining, desalination and food industries . Horizontal Tube Evaporator (HTE) is an important thermal desalination device, where boiling takes place in a thin film on horizontal tubes. Many investigators show that, the world dependence on desalination increases greatly in the last twenty years. Sea water desalination seams to be the best solution for the water shortage problem.

Many investigators studied the boiling heat transfer from theoretical and experimental point of view [1-9]. Experimental and theoretical work of H. M. Mostafa [1] for boiling heat transfer in a thin film on horizontal tube heated by a waste steam. W. H. Parken et al [3] studied the same problem using electrically heated tubes . P. K. Tewari [5] studied the nucleate boiling in a thin film on horizontal tube at atmospheric and sub-atmospheric pressures by using distilled and Sodium Chloride solutions.

Heat transfer for saturated falling-film evaporation on a horizontal tube has been analytically and experimentally studied by M. C. Chyu and A. E. Bergies [6] . The effect of film flow rate, liquid feed height and wall superheat are investigated. Two models have been proposed, both models based upon three defined heat transfer regions, the jet impingement region, the thermal developing region and the fully developed region. Both two models assumed heat is conducted across the film and evaporation takes place at the free surface. The influence on heat transfer coefficient is even smaller at low Renynolds number and independent of Reynolds number at high heat flux (208 $KW/m^2$). Both models and experimental data demonstrate, that heat transfer coefficient is independent on wall superheat.

Theoretical analysis was performed by D. Moalem and S. Sideman [8] to study the overall heat transfer coefficient in a horizontal evaporator- condenser tube for low heat flux in laminar flow regime. Local evaporation heat transfer coefficient around the tube has a maximum value at angle equal to $\Pi/2$ from the top because the film thickness was a minimum at this angle. In laminar flow regime the average overall heat transfer coefficient decrease with increasing Reynolds number or increasing tube radius.

## 2- GOVERNING EQUATIONS

Fig.(1-a) shows the system of coordinate used to analyze, mathematically, the present problem. According to the present proposed model some assumptions are made. Hydrodynamic as well as thermal flow field are assumed to be identical along the tube length. The radial velocity is assumed to be very small compare to the tangential component. According to these assumption the energy equation in cylinderical coordinate is simplified to the form:

$$\frac{V}{r}\ \frac{\partial T}{\partial \phi} = \frac{K}{\rho C_p}\left(\frac{\partial^2 T}{\partial r^2} + \frac{1}{r}\ \frac{\partial T}{\partial r}\right) . \qquad (1)$$

with the boundary condition:

$$\text{at} \quad r=R_o \qquad T=T_v \quad ; \qquad (2)$$
$$\text{at} \quad r=R_o+\delta \qquad T=T_v \quad .$$

In equation (1), V is the average tangential component of the velocity which is determined according to the relation:

$$V = \Gamma / \rho\, \delta_o \qquad (3)$$

Where $\Gamma$ is the rate of falling water per unit length of the tube per one side ( $\Gamma = m^{\cdot}/2L$ ) and $\delta_o$ is the film thickness at the position $\phi=0.0$ and is approximated by

$$\delta_o = A_o / ( 2\ L ) \qquad (4)$$

The film thickness $\delta$ at general position $\phi$ is estimated with the aid of the equation;

$$\delta = \delta_i \, EXP(-q'' R_o \Phi / \Gamma h_{fg}) \qquad (5)$$

Equation 5 is derived according to the mass balance of the evaporation process from the free surface of the film (Figure (1-b)).

To put flow describing equations (1-5) in dimensionless form, one defines the following dimensionless independent and dependent variables as follows:

$$R = r/R_o \quad : \quad \Phi = \phi / \phi_o \quad : \qquad (6)$$
$$\delta = \delta / R_o \quad : \quad \theta = (T - T_v)/(T_w - T_v) \quad .$$

With the aid of the foregoing definitions of variables (equations (6)), the dimensionless form of energy equation , can be written as:

$$\frac{1}{R} \frac{\partial \theta}{\partial \Phi} = (4\Pi/Re*Pr)*(\dot{\delta}_o) \left[ \frac{\partial^2 \theta}{\partial R^2} + \frac{1}{R} \frac{\partial \theta}{\partial R} \right] \quad . \qquad (7)$$

With the boundary condition:

$$\text{at } R = 1 \quad : \quad \theta = 1 \quad :$$
$$\text{at } R = 1 + \dot{\delta} \quad : \quad \theta = 0.0 \quad . \qquad (8)$$

Where Re & Pr are Reynolds and Prandtl numbers , which have the following definitions:

$$Re = 4\Gamma/\mu \quad : \quad Pr = \mu C_p / K \quad . \qquad (9)$$

Solving equations (7-9), the temperature distribution through out the flow field can be evaluated and, in turn, one calculates the local heat transfer coefficient by using the local heat flux and wall superheat as follows:

$$h_\phi = q''_{v,\phi} / (\Delta T)_{sup} \quad . \qquad (10)$$

The local heat flux at the wall is calculated according to the equation:

$$q''_{v,\phi} = - K * (\Delta T)_{sup} * (\partial\theta/\partial R)_1 / R_o \qquad (11)$$

Where $(\partial\theta/\partial R)_1$ is the gradient of the dimensionless temperature at the tube wall.

The average boiling heat transfer coefficient is calculated through the following relation:

$$h = \frac{1}{\Pi} \int_o^\pi h_\phi \, d\phi \qquad (12)$$

**3- NUMERICAL PROCEDURE**

The dimensionless energy equation and its boundary conditions equations (7-9) are solved numerically, using finite divided difference method. As shown in Fig. (1-c) R-Φ flow field is covered with a mesh, their nodes are identified by the identifier [illegible] any position [illegible] the [illegible] [illegible]

$$R_i = [illegible] (i-1)\Delta R \qquad [illegible] = (j-1)\Delta\Gamma$$

where $\Delta R$ and $\Delta\Gamma$ are the step size in radial and [illegible] directions respectively. Taking n as the total number of [illegible] in radial direction, the step size in this direction is [illegible] as:

$$\Delta R = [illegible] (n-1) [illegible]$$

The derivatives of the variable $\theta$ with respect to $R, \Gamma$ can be approximated by the following finite divided differences as

$$\partial\theta/\partial R = [illegible]$$
$$\partial^2\theta/\partial R^2 = [illegible] - 2\,\theta [illegible] + \theta [illegible] / \Delta R^2 \qquad (3)$$
$$\partial\theta/\partial\Gamma = [illegible] - \theta [illegible] / \Delta\Gamma$$

Substitution of the approximate derivatives in the [illegible] equation leads to the following set of linear algebraic equations:

$$[illegible] + [illegible] + [illegible] = A [illegible] \qquad (4)$$

where the coefficients of the [illegible] [illegible] (4) are defined as:

$$i = 1, 2, \ldots, n$$
$$C = [illegible]$$
$$[illegible]$$
$$[illegible] \qquad (5)$$
$$A = [illegible]$$

[illegible] are of the tri-diagonal matrix [illegible] tri-diagonal matrix equations are solved [illegible] substitution technique. The solution of equations [illegible] [illegible] in iterative manner [illegible] [illegible] achieved. A computer program is designed and [illegible] to predict the temperature profile across film thickness and local heat flux. And thus local and average boiling heat transfer coefficient and Nusselt number can be calculated.
The suitable total number of nodes in both R and $\Gamma$ directions are found to be [illegible].

## 4- RESULTS AND DISCUSSION

The dimensionless thickness for the evaporating film around the tube circumference is shown in Fig. [illegible]. The film thickness decreases with the angular position specially for smaller values of Reynolds number. The developing of the temperature profile becomes more and more linear with angular position and it is very close to linear distribution for [illegible] as shown in Fig. (3). This [illegible] is in good agreement with the results obtained by M. [illegible] and A. E. Bergles [illegible]. The local heat flux decreases with the angular position as shown in Fig. (4). It is clear that the local heat transfer coefficient and local Nusselt number have the highest value at the top of the tube and then decrease rapidly till they has an asymptotic values (starting from $\phi = \pi/4$

The effect of mass flow rate (or Reynolds number) on the Nusselt number is shown in Fig. (5). It is found that Reynolds number has a little effect on local Nusselt number specially at higher angular position.

The effect of tube diameter on the heat transfer coefficient is studied as shown in Fig. (6). From this figure it is clear that the heat transfer coefficient increases with decreasing tube diameter in laminar flow.

In laminar flow (Re<750) the average Nusselt number increases with increasing Reynolds number , as shown in Fig (7). The amount of liberated vapor from the water film is significant for low Reynolds number (smaller film thickness) and thus a relative rapid decrease in the film thickness with the angle $\phi$ is expected. This causes an increase in the local boiling heat transfer coefficient and local Nusselt number , specially at higher degree of superheat .

Fig. (8) shows a comparison between the present results and M. C. Chyu et al (6). A good agreement between the two models proposed by M. C. Chyu et al and present work is found

A comparison between the average boiling heat transfer coefficient obtained from theoretical results and experimental results obtained by Mostafa. H. M.[1] is shown in Fig. (9). The difference between the experimental and theoretical results is probably due to the nonuniform spread of water along the tube circumference. Moreover in experimental work , a fraction of the total area is covered by a relatively thin film where as in other parts the flow is turbulent and or wavy. Also, the non-uniform rain-like drops falling on the tube may enhance the transfer rate by initiating concentric waves. These effects are not accounted in theoretical work. For these reasons the experimental heat transfer coefficient is greater than the theoretical one by about 17% at the same working conditions.

## 5- CONCLUSION

In this study a model describing the boiling heat transfer process over a horizontal tube at constant wall temperature is proposed. To check the validity of this model, a comparison between the obtained results with that of the previous work proved the validity of this model. It is found that the boiling heat transfer coefficient increases with decreasing tube diameter. Also increasing wall superheat, heat flux and Reynolds number cause an increase in boiling heat transfer coefficient.

**ACKNOWLEDGEMENT**

The authors wishes to express his gratitude to Prof. Dr. H. M. El-Saadany and Prof. Dr. M. M. Mahgoub for his continuing advice and encouragement.

**NOMENCLATURE**

| | | |
|---|---|---|
| $A_o$ | Distributer orifice area | $m^2$ |
| D | Diameter | m |
| h | Average boiling heat transfer coefficient | $W/m^2.°C$ |
| $h_\phi$ | Local boiling heat transfer coefficient | $W/m^2.°C$ |
| $h_{fg}$ | Latent heat of evaporation | $J/kg.°C$ |
| I | Increment in nodes in r-direction | — |
| J | Increment in nodes in $\phi$-direction | — |
| K | Thermal conductivity | $W/m.°C$ |
| L | Tube length | m |
| m | Number of nodes in $\phi$-direction | — |
| $\dot{m}_{cir}$ | Circulated mass flow rate | kg/s |
| n | Number of nodes in r-direction | — |
| q" | Heat flux. | $W/m^2$ |
| r | Radial coordinate | m |
| $R_o$ | Outer tube radius | m |
| R | Dimensionless tube radius | — |
| T | Temperature | °C |
| $T^*$ | Saturation temperature of waste steam | °C |
| $\Delta T_{sup}$ | Superheat temperature difference $(T_w-T_v)$ | °C |
| $U_o$ | Velocity of free falling film | m/s |
| u | Radial velocity | m/s |
| V | Tangential velocity | m/s |
| Z | Axial coordinate of the test tube | m |

**Greek symbols:**

| | | |
|---|---|---|
| $\Gamma$ | Mass flow rate per unit length per one side of the tube | kg/m s |
| $\delta$ | Film thickness | m |
| $\theta$ | Dimensionless temperature difference$=(T-T_v)/(T_w-T_v)$ | — |
| $\mu$ | Dynamic viscosity | $N.s/m^2$ |
| $\nu$ | Kinematic viscosity | $m^2/s$ |
| $\rho$ | Density | $kg/m^3$ |
| $\varphi$ | Angle of inclination | Rad |
| $\Phi$ | Angular position | — |

**Subscripts:**

| | |
|---|---|
| c | Condensate |
| L | Liquid |
| o | Orifice, outer, initial |
| s | Steam |
| sup | Superheat |

v Vapor
w Wall

**Dimensionless numbers:**

Nu Nusselt Number (hD/K)
Pr Prandtl Number ($C_p.\mu/K$)
Re Reynolds Number ($4\Gamma/\mu$)

**REFERENCES**

1-H. M. Mostafa (Boiling heat transfer in a thin film on horizontal tubes) Ph.D. Thesis, El-Mansoura University , 1994.

2-S.Zhang and G.Gogos (Film evaporation of a spherical droplet over a hot surface ;fluid mechanics and heat /mass transfer) J.Fluid Mechanics, Vol.222, pp. 543-563., 1991.

3-W.H.Parken, L.S.Fletcher, V.Sernas and J.C.Han (Heat transfer through falling film evaporation and boiling on horizontal tubes) ASME Journal Of Heat Transfer Vol.112, pp. 744-750. Aug. 1990.

4-S.G.Bankoff (Dynamics and stability of thin heated liquid film) ASME Journal Of Heat Transfer Vol.112, pp. 538-546. Aug. 1990.

5-P.K.Tewari, P.K.Verma and and M.P.S. Ramini (Nucleate boiling in a thin film on a horizontal tube at atmospheric and sub-atmospheric pressures) Int. J. Heat Mass Transfer, Vol. 32 ,No. 4 ,pp.723-728 ,1989.

6-M.C.Chyu and A.E.Bergles (An analytical and experimental study of falling film evaporation on a horizontal tube ) ASME Journal Of Heat Transfer Vol. 109, pp. 983-990 ,Nov, 1987.

7-K. Edahiro, T. Hamada, M. Arai and Y. Hirao (Research and development of multi-effect horizontal tube film evaporator) Desalination. Vol.22, pp.121 ,1977.

8-D.Moalem and S.Sideman (Theoretical analysis of a horizontal condenser-evaporator tube) Int. J. Heat Mass Transfer. Vol. 19 ,pp. 259-270 ,1976.

9-S.Sideman, D.Moalem and R.Semiat (Theoretical analysis of horizontal condenser-evaporator conducts of various cross sections) Desalination Vol.17, pp. 167-192, 1975.

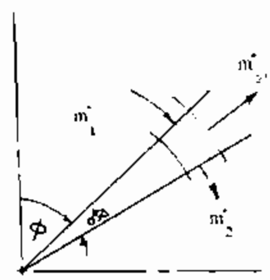

(1.a) Mass balance of differential element

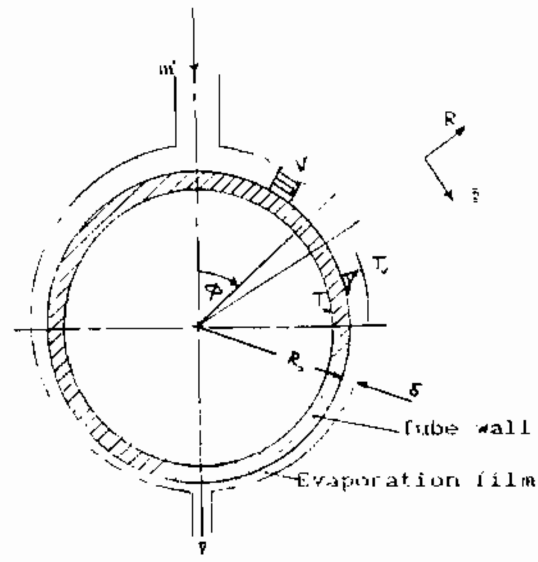


(1.b) Test tube co-ordinates system

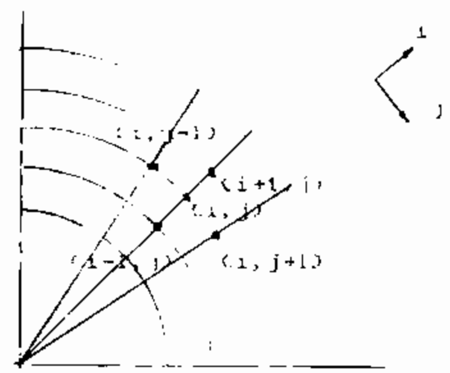


(1.C) The used mesh in calculating procedure

Fig.(1) Schematic description of the flow field

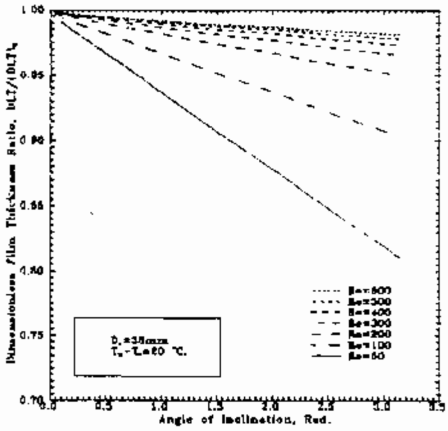


Fig.(2)Variation of the theoretical dimensionless water film thickness around the test tube for laminar flow.

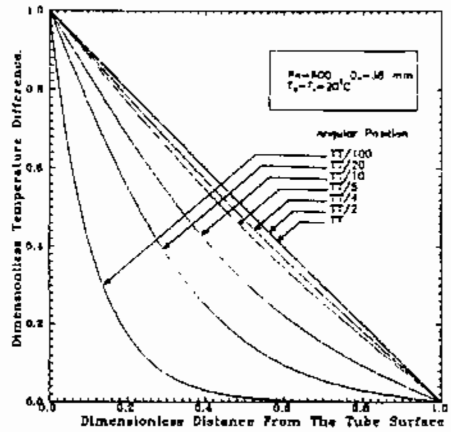


Fig.(3) Theoretical temperature profile across water film at different angular position.

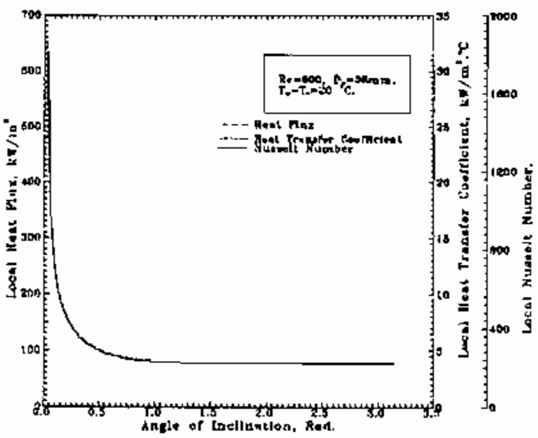


Fig.(4)Distribution of local heat flux ,Nusselt number and heat transfer coefficient versus angular position.

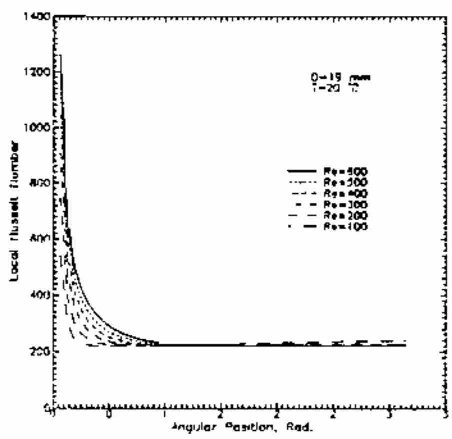


Fig.(5) Distribution of local Nusselt number versus angular position for laminar flow

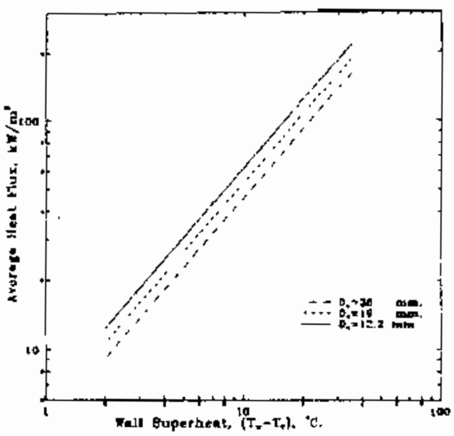


Fig.(6) Boiling curve for laminar flow (Re=500) at various tube diameters

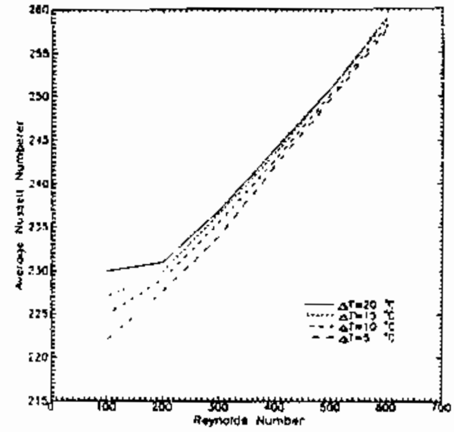


Fig.(7) Effect of wall superheat on the average Nussalt number in laminar flow ($D_o$=19 mm)

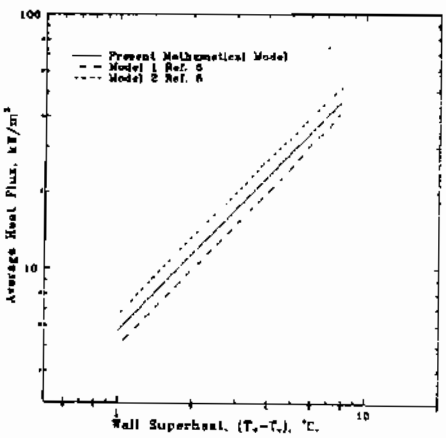


Fig.(8) Copmarison between prsent results with previous data for laminar flow.

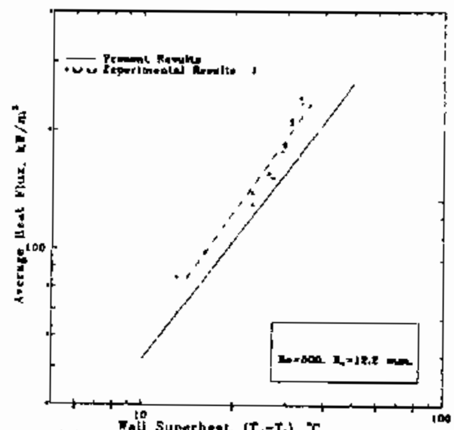


Fig.(9) Boiling curve for present theoretical results and another experimental results 1 in laminar flow

# UTILIZATION OF SOLAR AIR HEATING FOR DRYING AGRICULTURAL PRODUCTS

**H. D. Ammari and G. I. Bisharat**
**Faculty of Engineering, Mu'tah University, Jordan.**

استخدام الهواء المسخن بالطاقة الشمسية لتجفيف المتوجات الزراعية

ملخص

تبحث هذة المقالة فى جدوى الاستفادة من تسخين الهواء بالطاقة الشمسية لتجفيف المتوجات الزراعية فى الاردن. تم استخدام اجهزة مجمعات للطاقة الشمسية ذات صفائح منبسطة كنموذج محاكاة لتقدير احمال مختلفة للتجفيف مع الأخذ بعين الاعتبار الاحوال الجوية فى الاردن. واستخدم اسلوب المحاكاة بواسطة الحاسوب لتقدير نسبة التغطية للطاقة الشمسية لأحمال التجفيف المعتادة معتمدا على حجم و خواص المجمعات الشمسية. واشارت النتائج بأن أكبر نسبة تغطية ممكنة لأحمال التجفيف وصلت ٤٩٪ ولكنها لم تزد عن ٤٣٪ عند استخدام مجمعات شمسية ذات كفاءة متدنية.

## ABSTRACT

The feasibility of solar energy utilization for drying agricultural products in Jordan is explored. A system of flat-plate solar collectors was used as a simulation model to investigate various typical thermal drying loads, taking into consideration the typical meteorologieal conditions in Jordan.

A eomputer simulation was used for the determination of the solar energy percentage coverage of typical thermal loads as a function of the size and properties of the collectors. The results obtained indicated that the percentage coverage of the typical thermal loads reached as high as 49%, but could not be in excess of 43% when relatively inexpensive collectors were used.

## INTRODUCTION

Solar energy seems to be regarded by many scientists as the only viable alternative to the present sources of energy. At present, however, only a minute proportion of the world's energy requirement is met by solar power. Nevertheless, the experts are placing their faith mainly in the enormous energy potential of the sun.

Solar energy can be harnessed in many ways. It can be used for space heating and cooling, domestic hot water heating , industrial process heating, and electricity generation. Here, however, the possibility of applying solar energy using flat-plate air collectors for drying agrieultural products in Jordan is examined. Drying agricultural products using conventional fuels results in eonsumption of large fuel quantities. On the other hand, traditional drying by exposing the agricultural produets to direct solar radiation in the field involves long drying periods, contamination, and degradation or losses of the product due to unexpected weather conditions. Thus, solar energy appears to have a good potential in this field.

Heating of process air for drying agricultural products using flat-plate air collectors was studied by Maroulis and Saravacos [1] The air-heating system was combined with a thermal storage bed employing concrete balls as bed material. Their work was concerned with the possibility of eovering typical thermal drying loads with regard to meteorological conditions in Greece. The solar coverage was determined as a function of the total surface area of the collectors and the thermal storage bed volume. Their evaluation was based on typical values of the properties of the collectors and the thermal storage bed. However, the effect of the collectors quality used on the efficiency of the system was not examined.

The evaluation in this work is pertinent to solar radiation in Jordan and is also for a system of flat-plate air collectors. But, various thermal drying loads were studied and a more sophisticated mathematical model for the collector was applied.

## SYSTEM DESCRIPTION

The solar air-heating system proposed consists of a series of air-collectors connected in parallel, which are combined with a typical dryer and a heat-recovery system as shown in Fig. 1. A centrifugal fan is used for circulating the preheated air. The system can operate in two modes, the decision being made with the use of a controller. According to the first mode which is active when there is sufficient insolation, the air is heated at the solar collectors. According to the second mode of operation the solar heating system is bypassed. Such system can be operated for 10 to 12 hours daily during the summer months in Jordan.

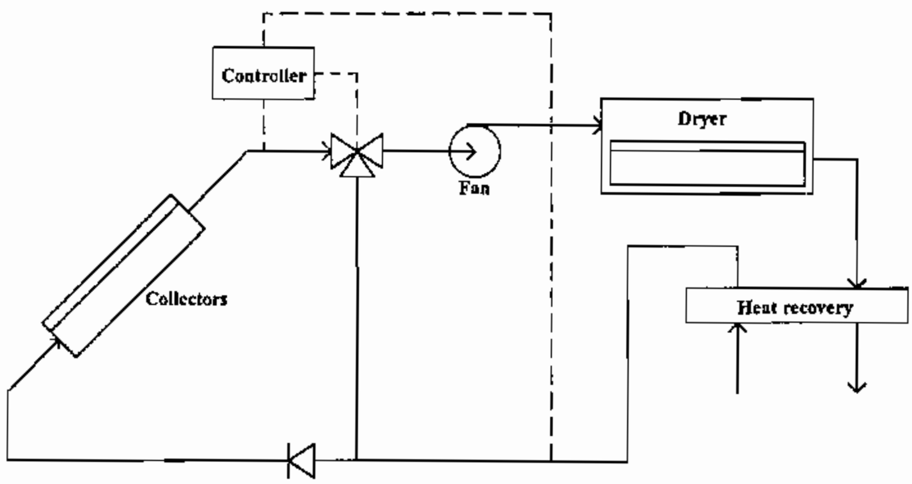


Fig. 1. Solar air-heating system with dryer and heat recovery.

The required thermal drying load is dependent upon the type of the dried product. Fruits and vegetables require a drying air temperature of 50 - 80°C and a relatively high air flow rate of about 1 $m^3/s$. Whereas, the drying of cereals requires a lower air temperature and flow rate. Furthermore, most agricultural products are harvested and dried during summer, when solar radiation is high. Thus, solar energy is best applied during summer for drying agricultural products. Typical thermal drying loads for the summer period are shown in Table 1.

As for the purpose of this work, a continuous 24 hours per day drying is assumed, applied throughout the six summer months of a typical year [2], from April to September. The desired air temperature at the dryer is chosen to be 60 or 80°C at a rate of 1 $m^3/s$. The inlet air temperature is assumed to be 40 or 24°C for Amman area whether a heat-recovery system is used or not, respectively. A heat-recovery system may utilize the exhaust air from the dryer for warming up the entering fresh air to the air-heating system.

Table 1. Thermal drying loads of agricultural products (air flow rate is constant at $1 m^3/s$ for 24 hours operation a day during the six summer months )

| Type of duty | Temperature of available air (°C) | Desired air temperature (°C) | Total thermal load (GJ / Summer) |
|---|---|---|---|
| D2460* | 24 | 60 | 680.6 |
| D4060 | 40 | 60 | 358.9 |
| D2480 | 24 | 80 | 1058.7 |
| D4080 | 40 | 80 | 717.8 |

*Duty type with temperature of available air of 24°C and desired air temperature of 60°C.

## SYSTEM SIMULATION

The Klein-Duffie-Beckman mathematical model [3] which was based on Close's model [4] was used. The model takes into account the collector heat capacity for the simulation of the thermal behavior of a flat-plate air collector.

According to this model the collector as a lumped system operates with a mean temperature $T_m$ and an equivalent heat capacity $C_A$.

When air circulates in the collector,

$$C_A \frac{d\,T_m}{dt} = F'[(\tau\alpha)_e G - U_L(T_m - T_a)] - \frac{m_c c_p}{A_c}(T_{co} - T_{ci}) \qquad \{1\}$$

When there is no air circulation in the collector,

$$C_A \frac{d\,T_m}{dt} = (\tau\alpha)_e G - U_L(T_m - T_a) \qquad \{2\}$$

Taking linear temperature distribution across the collector. That is,

$$T_m = (T_{co} + T_{ci}) / 2 \qquad \{3\}$$

where, $m_c$ is the mass air flow rate at the collector,
$c_p$ is the air heat capacity,
$G$ is the incident solar radiation at the collector,
$A_c$ is the surface area of the collector, and
$T_{ci}$, $T_{co}$ are the collector inlet and outlet air temperatures respectively, and
$T_a$ is the ambient air temperature.

According to this model the collector operation is dependent upon the following characteristics :

i . Plate efficiency factor F',
ii . Effective transmittance-absorption product $(\tau\alpha)_e$,

iii . Overall coefficient of heat losses $U_L$, and
iv . Equivalent heat capacity $C_A$.

The mathematical model is complemented by the following equations:

$$m_c = \gamma\, m_D \tag{4}$$

$$T_o = \gamma\, T_{co} + (1 - \gamma)\, T_i \tag{5}$$

where, $m_D$ is mass air flow rate to the dryer,
$T_i$, $T_o$ are the inlet and outlet temperatures at the solar heating system respectively, and
$\gamma$ is a variable whose value is related to the function of the controller as follows:

$$\gamma = \begin{cases} 1 & \text{if} \quad T_{co} > T_{on} \\ \gamma_o & \text{if} \quad T_{off} \leq T_{co} \leq T_{on} \\ 0 & \text{if} \quad T_{co} < T_{off} \end{cases}$$

where, $\gamma_o$ is the previous timewise decision function of the controller, and
$T_{on}$, $T_{off}$ are the controller dead bands, °C.

The mathematical model of the solar air-heating system was solved using computational numerical methods with a step size of 10 minutes for the time.

## METEOROLOGICAL DATA

Jordan is blessed with high level of insolation over all of its regions. The abundance of solar energy in Jordan is evident from the annual daily mean global solar irradiance on a horizontal surface which ranges between 5 and 7 kWh/m$^2$ compared to that of Europe and most of North America that amounts to 3.5 kWh/m$^2$. The excellent irradiance in Jordan corresponds to a total annual of 600-2300 kWh/m$^2$. In addition, the sunshine duration is with an average of 9 hours a day and 330 sunny days per year.

Mean daily values of solar radiation (G) and ambient temperature ($T_a$) of the typical solar year [2] were used in the calculations. The typical solar year was estimated from the meteorological data of the Amman area, representing the highland and plateau region of Jordan, for the five-years period, 1990 - 1994. Figs. 2 and 3 show the variation of $T_a$ and G during the typical year, respectively. As for the collectors tilt angle, measurements made by El-Kassaby [5] have indicated that the optimum tilt angle in summer (from day 81 up to day 265) for Amman area is zero where overall maximum radiation can be obtained. El-Kassaby's measurements were verified with some theoretical analysis. Nonetheless, the Liu-Jordan method [6] can be used for the conversion of radiation data from a horizontal to an inclined surface.

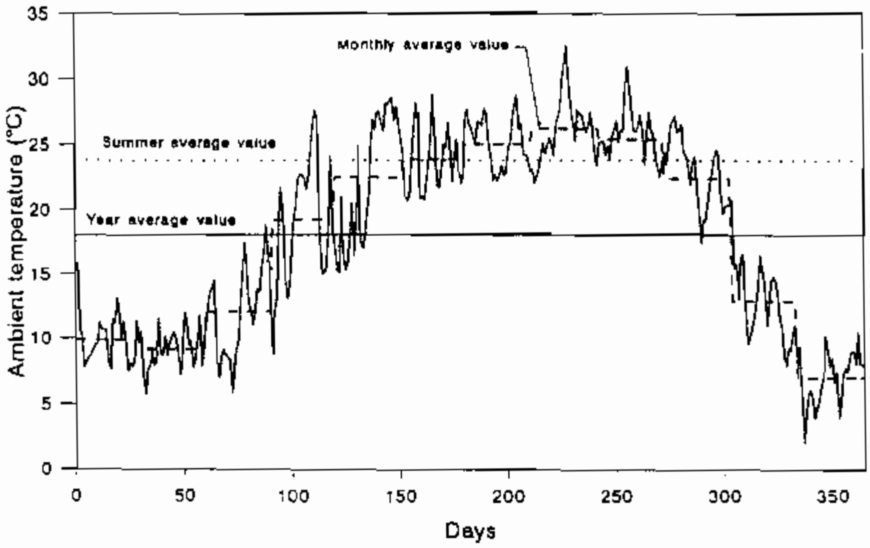


Fig. 2. Mean daily ambient temperature during a typical year (Amman region).

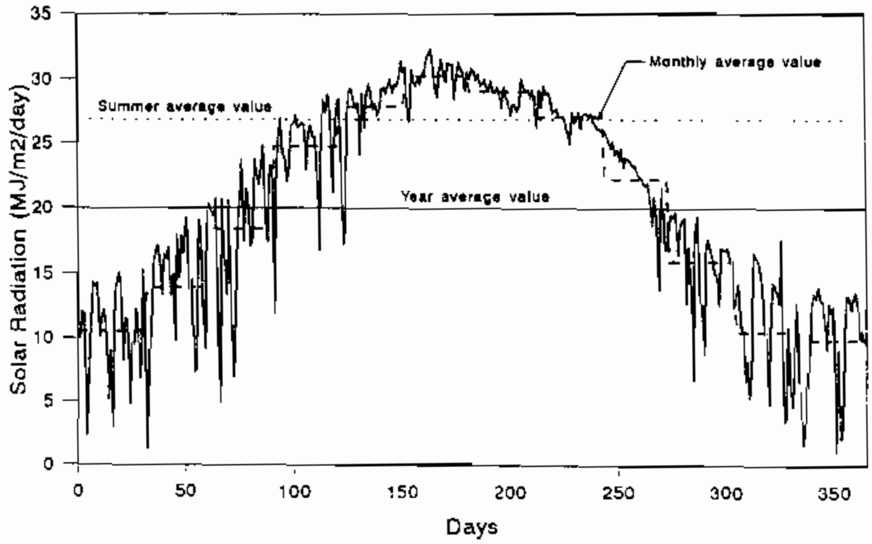


Fig. 3. Mean daily solar radiation on a horizontal plane during a typical year (Amman region).

The estimated typical year yields the mean daily values of G and $T_a$, but it does not provide any information about the variation of these quantities during each day, which is required for a detailed simulation of the solar air-heating system. The daily variation of G and $T_a$, can be expressed by the following equations [1]:

$$T_a(t) = \frac{T_{a,min} + T_{a,max}}{2} - \frac{T_{a,max} - T_{a,min}}{2} \cos\pi\left(\frac{t - t_{SR}}{12}\right) \quad (7)$$

$$G(t) = \frac{\pi G}{2(t_{SS} - t_{SR})} \sin\left(\pi \frac{t - t_{SR}}{t_{SS} - t_{SR}}\right)\left[1 + \lambda \sin\left(2\kappa\pi \frac{t - t_{SR}}{t_{SS} - t_{SR}}\right)\right] \quad (8)$$

where,

$T_a$ (t) and G(t) are the ambient temperature and solar radiation at time t [$0 < t < 24$],

$T_{a,min}$ and $T_{a,max}$ are the minimum and maximum temperatures during a day respectively, and

$t_{sr}$ and $t_{ss}$ are the sunrise and sunset times respectively.

The frequency of clouding is expressed by the integer parameter $\kappa$ and the density of clouds by the parameter $\lambda$ [$0 < \lambda < 1$]. The parameters $\kappa$ and $\lambda$ are chosen as representative values for the region of proposed solar installation.

## RESULTS AND DISCUSSION

***Simulation of the proposed solar system***

In the case of thermal duty D2460 given in Table 1 and with values of the design parameters shown in Table 2, the results of the system simulation are those shown in Figs. 4, 5 and 6.

Table 2. Values of the design parameters of the proposed air-heating system

| | |
|---|---|
| Total surfaee area of collectors $A_c$ | 200 $m^2$ |
| Angle of tilt of collectors (opt. for summer) | $0^\circ$ |
| Equivalent heat capacity of collector $C_A$ | 10 $kJ/m^2$ K |
| Plate efficiency factor F' | 0.8 |
| Transmittance-absorption product $(\tau\alpha)_e$ | 0.75 |
| Overall coefficient of thermal losses $U_L$ | 8 W / $m^2$ K |
| Controller characteristics $T_{on}$ | $60^\circ$ C |
| $T_{off}$ | $40^\circ$ C |

The daily system useful thermal energy, $q_{us}$, that is utilized at the dryer temperature of 60°C, the daily energy of the air stream at the outlet of the collector, $q_{co}$, and the daily incident solar energy to collectors, $q_{inc}$, each per month are displayed in Fig. 4. Note that the difference between $q_{co}$ and $q_{us}$ is the rejected thermal energy from the system, which is provided at temperatures higher than desired. Since considerable solar radiation occurs during June, the maximum useful energy of the system is attained in this month, at which time the rejected energy is greatest. The excess energy can be utilized by using a thermal storage unit which would extend the system operating time, or by mixing the hot air with available air such that the desired temperature is reached. The latter situation, however, would be accompanied by an increase of the air flow rate which would result in an increase of about 13% and 18.5% in the summer average system efficiency and summer average percentage coverage of the thermal duty, respectively

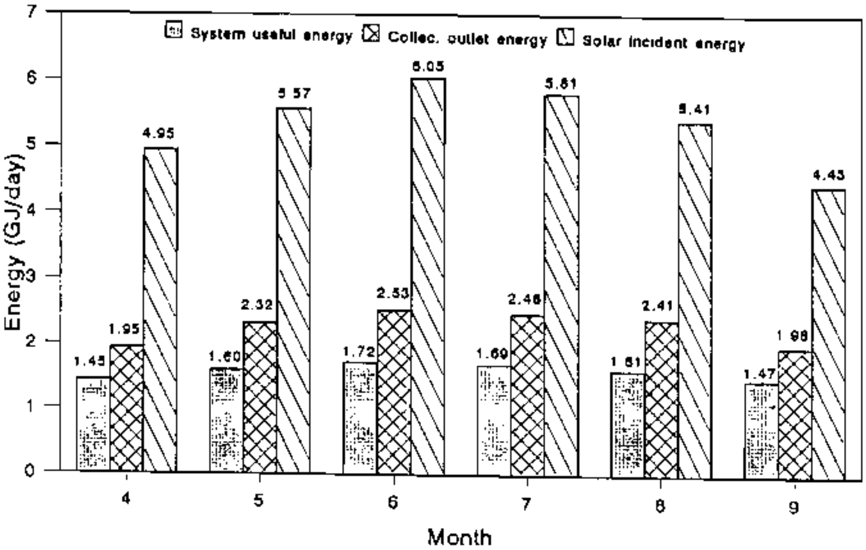


Fig. 4. Energy results of the simulated air-heating system for thermal duty D2460.

The daily percentage coverage and daily efficiency of the system for the thermal duty D2460 are shown in Figs. 5 and 6 respectively.

As can be seen from Fig. 5, the percentage coverage of the thermal duty amounts to 39-46% during summer which demonstrates the capability of the system during the period of high thermal load demands. The corresponding system thermal efficiency is 29-33% (see Fig. 6).

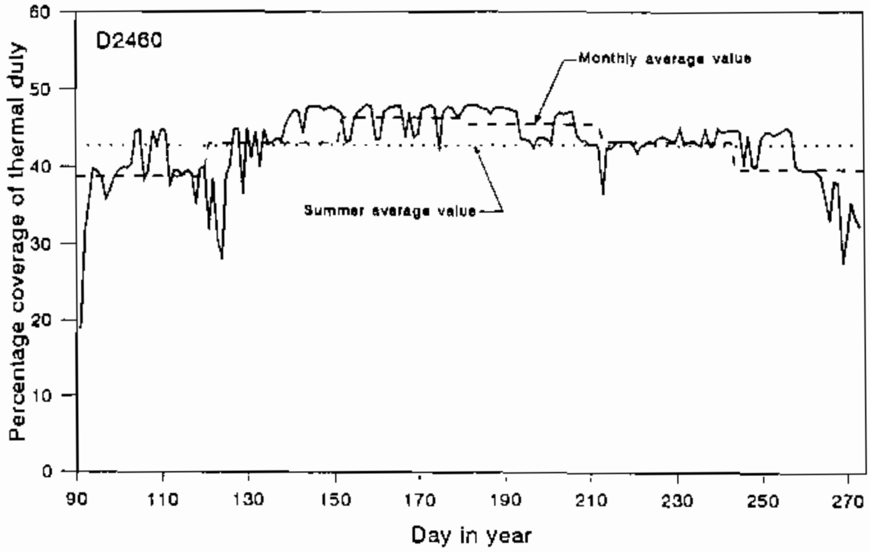


Fig. 5. Daily percentage coverage of thermal duty during a typical summer in Amman.

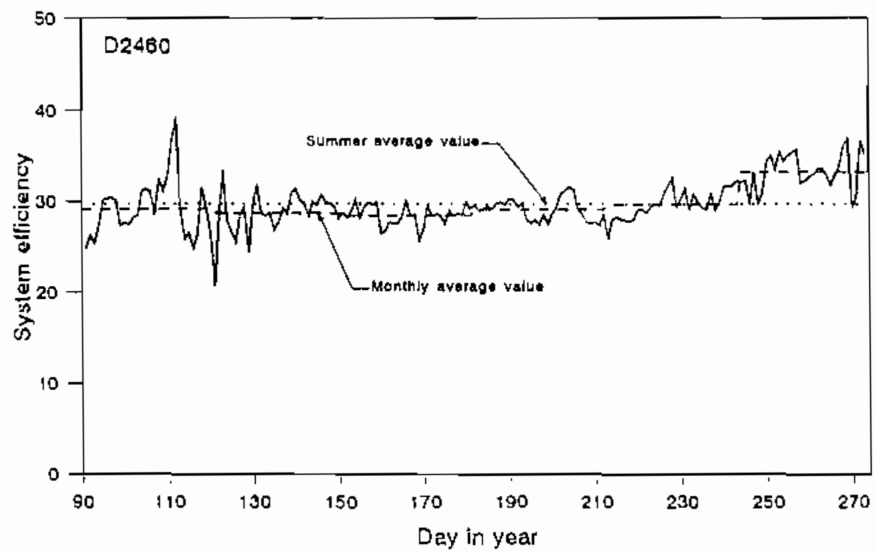


Fig. 6. Daily system efficiency during a typical summer in Amman.

*Effect of size and quality of collectors*

The percentage coverage of the thermal drying loads with solar energy defined in Table 1 is shown in Fig. 7 as a function of the total surface area of collectors for different values of collector parameters; the overall coefficient of thermal losses $U_L$; transmittance-absorption product $(\tau\alpha)_c$, and thermal efficiency factor F'. The total surface area of collectors was varied from 0 to 1000 m$^2$, the thermal heat losses coefficient from 6 to 10 W/m$^2$K, the transmittance-

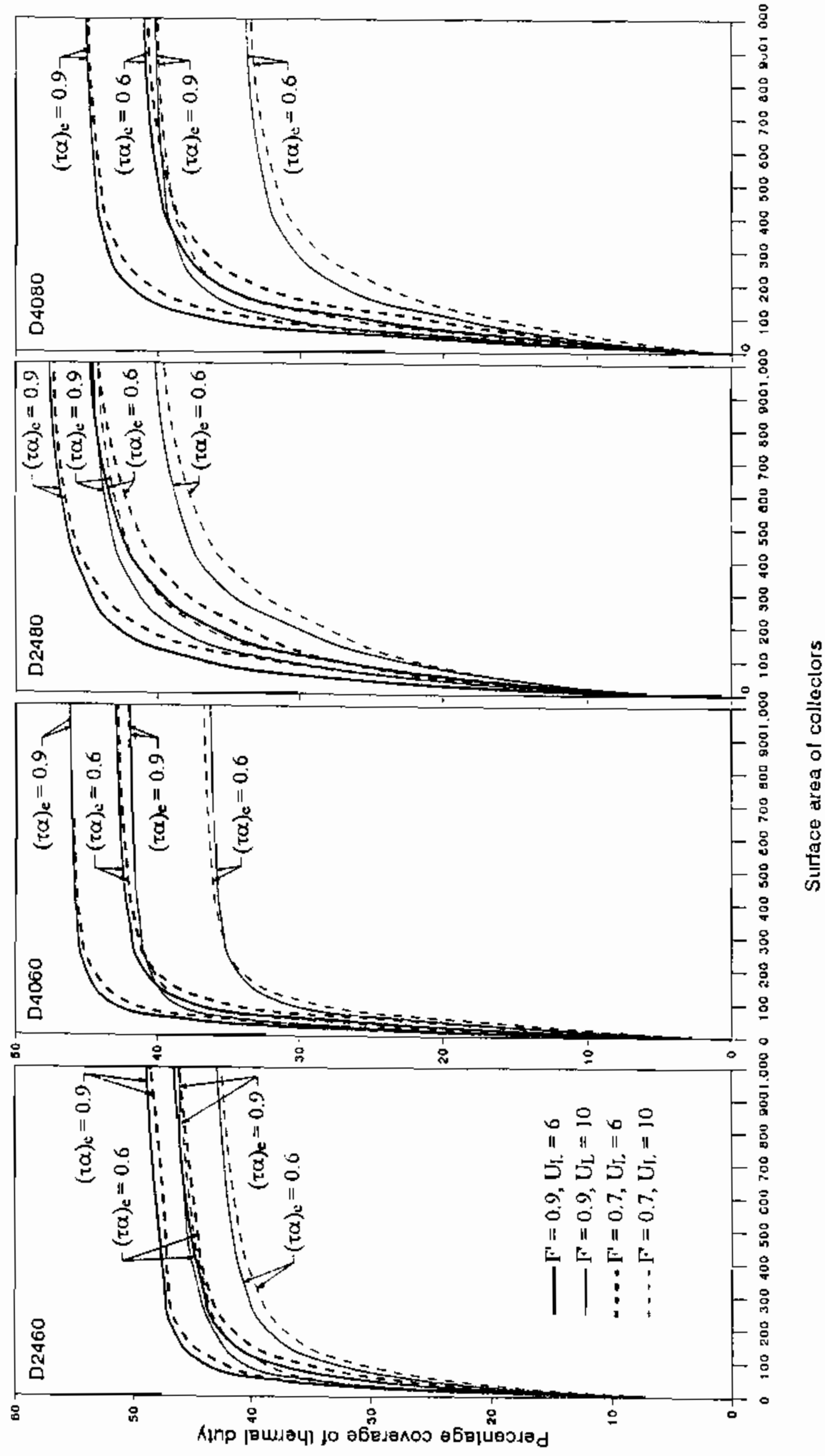


Fig. 7. Percentage coverage of thermal drying loads for drying agricultural products

absorption product from 0.6 to 0.9 and the plate efficiency factor from 0.7 to 0.9. All other design parameters were kept the same (see Table 2). Note that the figure is referred to the desired air flow rate of 1 $m^3/s$ which corresponds to a medium size drying unit. Generalization of the outcome for increased flow rates is possible, in which case the extensive properties of the system are increased accordingly while the intensive properties are kept constant.

As can be observed from Fig. 7, the effect of the overall coefficient of heat losses $U_L$ and the transmittance-absorption product $(\tau\alpha)_e$ on the percentage coverage of thermal duties is relatively significant; the variation considered in either $U_L$ or $(\tau\alpha)_e$ results in changes ranging from 4 to 7% in the coverage depending on the case studied. Whereas, the variation in the plate efficiency factor has somewhat negligible effect on the percentage coverage (mostly within 1%).

The simulation results indicate that using a collector with a good insulation ($U_L$ = 6 $W/m^2$ K) and a good absorption coefficient ($(\tau\alpha)_e$ = 0.9) results in 49% maximum coverage of the total thermal load. With a poor insulation ($U_L$ = 10 $W/m^2$ K) and lower absorption coefficient ($(\tau\alpha)_e$ = 0.6), the corresponding percentage coverage becomes 43%. But in any case the percentage coverage was always in excess of 33%.

It should be stressed also, that increasing the collectors surface area above 200 $m^2$ of a dryer operating at 60°C does not improve the capacity of the system substantially. For a dryer operating at 80°C, the corresponding surface area above which the system capacity is not substantially increased is 400 $m^2$.

## CONCLUSIONS

The simulation results of the solar air-heating system to cover the thermal duty on drying of agricultural products have provided the following conclusions:

1. The solar energy percentage coverage of thermal duties cannot in any case be in excess of 43% when inexpensive collectors of low $(\tau\alpha)_e$ and high $U_L$ are used, but is always in excess of 33%. However, the maximum percentage could be increased to 49% if expensive collectors are used.
2. The plate efficiency factor F' does not have a substantial influence on the percentage coverage of the thermal duties, in contrast to $(\tau\alpha)_e$ and $U_L$ which have a significant effect on the coverage.
3. An increase of the surface area of the collectors above a certain level, which is related to the thermal duty does not improve substantially the percentage coverage of the thermal duty due to high amounts of energy rejected.

## ACKNOWLEDGEMENT

The authors wish to express their gratitude to Jordan Meteorological Department and in particular Dr. Jaser Al-Rabadhi for their contribution in providing the meteorological data of Jordan.

**REFERENCES**

[1] Z. B. Maroulis and G. D. Saravacos, "Solar Heating of Air for Drying Agricultural Products", *Solar and Wind Technology*, Vol. 3, No. 2, pp. 127 - 134, 1986

[2] G. S. Raouzeous and D. E. Moissis, "Determining the Typical Year of Solar Radiation for Use in Models Simulating Solar Systems", International Conference on Passive and Energy Architecture, Crete , Greece 1983.

[3] S. A. Klein, J. A. Duffie and W. A. Beckman, "Transient Considerations of Flat- plate Collectors", ASME, *Journal of Engineering for Power*, pp. 109 - 113, 1974.

[4] D. J. Close, "A Design Approach for Solar Processes", *Solar Energy*, Vol. 11, p. 112, 1967

[5] M. M. El-Kassaby, "The Optimum Seasonally and Yearly Tilt Angle for South Facing Solar Collectors", *Alexandria Engineerig Journal*, Vol. 27, No. 4, pp. 103-130, 1988.

[6] B. Y. H. Liu and R. C. Jordan, "A Rational Procedure for Predicting the Long-Term Average Performance of Flat-Plate Solar-Energy Collectors", *Solar Energy*, Vol. 7, No. 2, pp. 53 - 74, 1963.